

From Random Walk to Multifractal Random Walk in Zooplankton Swimming Behavior

Laurent Seuront^{1,2,*}, François G. Schmitt¹, Mathew C. Brewer^{3,4}, J. Rudi Strickler⁴ and Sami Souissi¹

¹Ecosystem Complexity Research Group, Station Marine de Wimereux, Université des Sciences et Technologies de Lille, CNRS-UMR 8013 ELICO, F-62930 Wimereux, France

²School of Biological Sciences, Flinders University, GPO Box 2100, Adelaide 5001, Australia

³Great Lakes WATER Institute, University of Wisconsin-Milwaukee, 600 East Greenfield Ave., Milwaukee, WI 53204, USA

⁴Present address: Department of Zoology, University of Florida, Gainesville, FL 32611, USA

(Accepted March 15, 2004)

Laurent Seuront, François G. Schmitt, Mathew C. Brewer, J. Rudi Strickler and Sami Souissi (2004)

From random walk to multifractal random walk in zooplankton swimming behavior. *Zoological Studies* 43(2): 498-510. Herein, we investigate the statistical properties of the swimming behavior of two of the most common freshwater and marine zooplankters, the cladoceran, *Daphnia pulex*, and the copepod, *Temora longicornis*. Both species undergo a very structured type of trajectory, with successive moves displaying intermittent amplitudes. We present an original statistical procedure, derived from the fields of turbulence and anomalous diffusion and specifically devoted to the characterization of intermittent patterns. We then show that the swimming paths belong to "multifractal random walks", characterized by a nonlinear moment scaling function for distance versus time. This clearly differs from the traditional Brownian and fractional Brownian walks expected or previously detected in animal behaviors. More specifically, we have identified differential behaviors in the horizontal and vertical planes. This suggests the existence of reminiscence of diel vertical migration as a predator-avoidance strategy or differential swimming behaviors related to mating, feeding, or predator-avoidance strategies. We also compare the structure of the swimming paths to the multifractal behavior of microscale phytoplankton distributions demonstrated in turbulent environments, and briefly discuss the potential causes of the observed differences between *D. pulex* and *T. longicornis* swimming behaviors.

<http://www.sinica.edu.tw/zool/zoolstud/43.2/498.pdf>

Key words: Zooplankton, Random walk, Anomalous diffusion, Animal behavior, Multifractal.

Animals typically search for food, hosts, and sexual partners and avoid predators in complex, spatially and temporally structured environments. In zooplankton ecology, examples come from a wide spectrum of swimming behaviors related to the species, age, prey density, presence of a predator or conspecific, sex of individuals, and information imparted into the surrounding water by a swimming animal, including both chemical and hydromechanical stimuli. Moreover, environmental complexity affects the movement patterns of animals; recent advances have demonstrated the heterogeneous nature of physical and biological

patterns and processes at scales relevant to individual organisms (Seuront et al. 1996a b 1999 2002, Cowles et al. 1998, Seymour et al. 2000, Waters and Mitchell 2002, Waters et al. 2003). There is thus a genuine need to establish a reference framework that links pure behavioral observations, the qualitative and quantitative nature of environment complexity, and zooplankton trophodynamic hypotheses.

This reference framework could be provided by fractal analysis that recently has been proven to overcome the major limitations of most behavioral metrics which are intrinsically scale-depen-

*To whom correspondence and reprint requests should be addressed. Tel: 33-321992937. Fax: 33-321992901. E-mail: Laurent.Seuront@univ-lille1.fr/Laurent.Seuront@flinders.edu.au

dent (see Seuront et al. 2004 for a review on the subject). Fractal analysis has thus been successfully applied to a wide range of animal behaviors, ranging from movements of marine (Erlandson and Kostylev 1995) and terrestrial (Gautestad and Mysterud, 1993, Wiens et al. 1995) invertebrates, swimming paths of both freshwater and marine zooplankton (Coughlin et al. 1992, Bundy et al. 1993, Brewer 1996, Jonsson and Johansson 1997, Dowling et al. 2000, Seuront et al. 2004), and search paths of small (Cody 1971, Pyke 1981) and large (Van Ballenberghe 1983, Bascompte and Vilà 1997, Mouillot and Viale 2001) terrestrial and marine vertebrates.

The resulting (fractal) properties, often referred to as Brownian (random) motion (i.e., when the fractal dimension D equals the dimension of the embedding space d) and fractional Brownian motion (i.e., when $D < d$), and the related framework proposed to simulate zooplankton swimming behavior are implicitly based on a Gaussian distribution of the spatial increments of the trajectory (e.g., see Peitgen et al. 1992). This hypothesis, however, is untenable considering the highly intermittent character of distances traveled by zooplankton organisms (Fig. 1). Such distributions are characterized by a few dense values and a wide range of low-density values that highly significantly diverge from normality (by the Kolmogorov-Smirnov test, $p < 0.001$). Schmitt and Seuront (2001 2002) thus recently demonstrated that the norm of copepod displacements should rather be thought of as a multifractal random walk or multifractal anomalous diffusion, and subsequently introduced a new type of stochastic process reproducing these multifractal scaling properties.

In this paper, in order to illustrate the challenging difficulty in obtaining accurate records of the 3-dimensional (3D) displacement of aquatic organisms, we first briefly present 2 different, but conceptually similar, methods that permit the collection of 3D swimming data at both high spatial and temporal resolution and for long periods. We subsequently focus on the stochastic methods devoted to the identification and characterization of multifractal anomalous diffusion. Further, to put the concepts developed in this paper in an ecological context, they are applied to a set of high-resolution 3D swimming trajectories of two of the most common freshwater and marine zooplankters, the cladoceran, *Daphnia pulex*, and the copepod, *Temora longicornis*. We first characterize the multifractal structure of the 3D swimming paths of *T.*

longicornis and *D. pulex*, then compare their properties. We further analyze the properties of the 2D projections of the 3D swimming paths to ensure the isotropy of the swimming behaviors of *T. longicornis* and *D. pulex*.

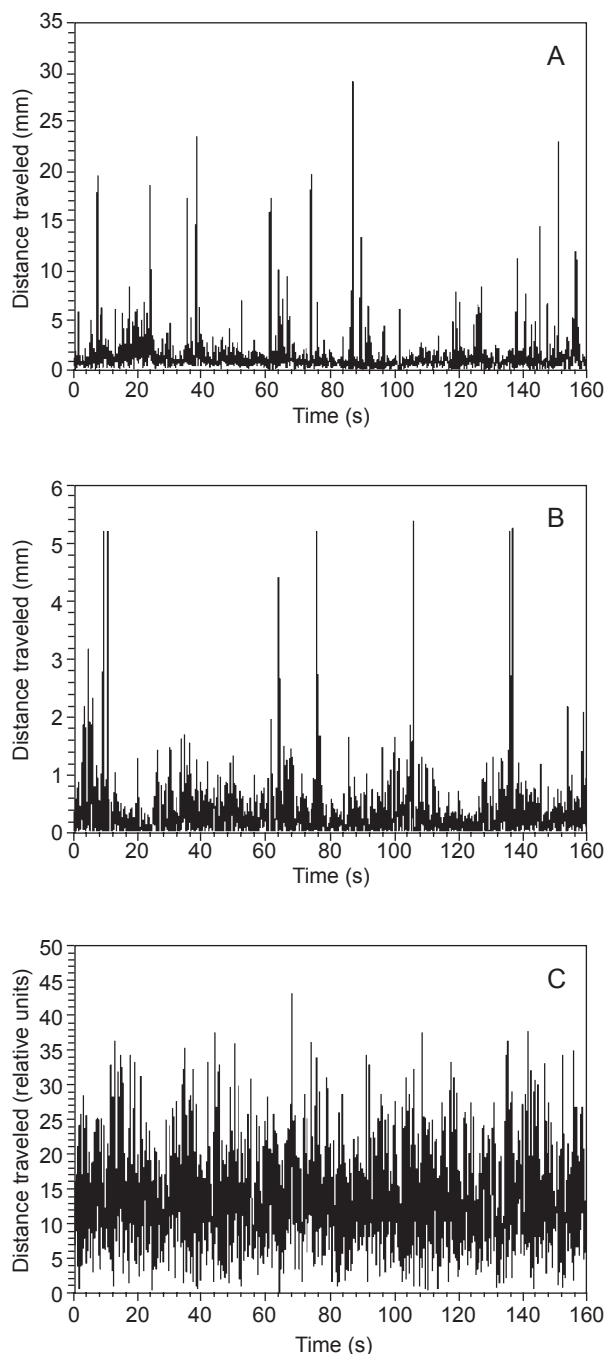


Fig. 1. Examples of distance traveled by *Temora longicornis* (12.5-Hz resolution; A) and *Daphnia pulex* (10-Hz resolution; B), compared to the distance traveled in the case of pure random motion (C).

MATERIALS AND METHODS

Living material collection and acclimation

Daphnia pulex

A clone of *Daphnia pulex* was cultured in aged tap water under cool white fluorescent bulbs, in a 16:8-h light-dark cycle. Cultures were maintained at the experimental temperature and fed every day with a 1:1 mixture of the green algae, *Ankistrodesmus* sp. and *Scenedesmus* sp., at a final concentration of about 5×10^5 cells/ml. Algae were grown in multiple 250 ml batch cultures under cool white fluorescent bulbs, in an 18:6-h light-dark cycle at 20°C in Bold's basal medium.

All recording experiments were carried out with animals swimming in an algal concentration of 5×10^4 cells/ml, which is an intermediate food concentration, well below *D. pulex*'s incipient limiting concentration (Lampert 1987). The test chamber was illuminated with a diffuse, fiberoptic light placed 0.5 m directly overhead that resulted in an illumination of about $12 \mu\text{E}/\text{m}^2/\text{s}$ in the vessel, approximately equal to full daylight. At least 1 h prior to the experiments, adult, gravid females (2.1 ± 0.2 mm) were transferred from their culturing vessels and acclimated to experimental light and food conditions in holding vessels. A single animal was then transferred from its holding vessel to the recording chamber with a large-bore pipette and allowed to acclimate for at least 10 min before recording began.

Temora longicornis

Individuals of the copepod, *Temora longicornis*, were collected with a WP2 net (200-mesh size) in offshore surface waters of the Eastern English Channel. Specimens were diluted in buckets using in situ water and transported to the laboratory. Acclimation of copepods consisted of being held in 20-L beakers filled with 0.45- μm -filtered seawater to which was added a suspension of the diatom, *Skeletonema costatum*, to a final concentration of 10^8 cells/l. Algae were grown in multiple 1-L batch cultures under cool fluorescent bulbs, in a 12:12-h light-dark cycle at 18°C in f/2 medium.

Prior to the filming experiment, adult females (1.1 ± 0.1 mm) were sorted by pipette, acclimated for 24 h at 18°C and fed on a mixture of the green alga, *Nannochloropsis occulata* (3 μm), and the flagellate, *Oxyrrhis marina* (13 μm). The larger heterotrophic flagellate, *O. marina*, was present as an additional food source. Illumination came from

two 75-W lamps (providing diffuse cold light) located above and below the container to ensure homogeneity of the light source and thus avoid phototropism. The illumination system was designed to provide a light intensity of around $10 \mu\text{E}/\text{m}^2/\text{s}$ in the vessel to be consistent with the *Daphnia* experiment. A single animal was sorted by pipette and left in the experimental filming setup to acclimatize for 15 min.

Recording the 3D behavior of swimming organisms

Daphnia pulex

All paths studied in this paper were movements of solitary *D. pulex* swimming in the 5-L (18 x 18 x 15.5 cm) Plexiglas recording vessel of the CritterSpy, a high-resolution 3D recording system. The CritterSpy uses a schlieren optical system consisting of a collimated red laser beam ($\lambda = 623$ nm) which serves as the light source for 2 orthogonally mounted video cameras, 2 frame number generators, two 50.8 cm (20-in) video monitors, and 2 VHS videocassette recorders (see Strickler 1985 and Bundy et al. 1993 for further details). This system simultaneously records orthogonal front (XZ) and side (YZ) views of the experimental chamber as dark-field images. To run the system, 2 operators view the camera images in real time. As the animal swims away from the center of either camera's view (marked with crosshairs on the monitors), 1 operator uses a trackball (X and Z dimensions) and the other a rotating cylinder (Y dimension) to bring the animal back into the center of both views. The actual re-centering of the image was achieved via 3 computer-controlled linear positioning motors (1 for each axis), that moved the entire optical system in response to the operators' input. A computer recorded the motor movements necessary to keep the animal centered in the 2 views as X, Y, and Z coordinates. Because the computer only recorded coordinates when the trackball or cylinder was moved, the coordinates were recorded at an uneven sampling rate (ranging from about 5 to 15 Hz). Paths were then interpolated to produce an even time interval (10 Hz) between successive position measurements. The 10 Hz rate is fast enough so that coordinates recorded at that temporal scale are the result of very small movements of the crosshairs corresponding to *Daphnia*'s characteristic hop-and-sink behavior.

Each individual *Daphnia* was recorded swimming for at least 30 min, after which the videotapes

were reviewed and valid segments were identified for analysis. Valid segments consisted of video in which an animal was swimming freely, at least 2 body lengths away from any of the chamber's walls or the surface of the water, and the animals were always within 1/2 body length of the crosshairs in the center of the video monitors. To ensure that there was a significant range of scales in each path, we only used paths that were at least 30 s in duration. After identifying valid sequences, the frame numbers imprinted on the video were used to isolate the corresponding time interval from the 3D coordinate data stored on the computer. These time series of coordinates are the 3D trajectories used in our analysis (Fig. 2, Table 1).

Temora longicornis

All paths considered here are the movements of solitary *T. longicornis* swimming in a 3.375-L (15 x 15 x 15 cm) glass recording vessel. The 3D trajectory of the copepod was recorded at a rate of 12.5 frames/s using 2 orthogonally focused and synchronized CCD black and white cameras (Hitachi KP M1, Japan; 875 x 560 pixels; focal distance, 17:53 mm), facing the front and side views of the experimental container. An encoder, RGB-PAL (Enc110 (For-A)), codes PAL-type red and green frames from the 2 instantaneous synchronized monochrome images. Each orthogonal view is then labeled and may be added to another at the

same time, t , to form 1 single color PAL-frame (see Schmitt and Seuront 2001 2002 for further details). The advantages of this frame superposition are to decrease hardware costs and to ensure optimal synchronization. The colored images were subsequently digitized (720 x 576 pixels), compressed, and stored in real time using a special acquisition card and appropriate software (PVR-Digital Processing Systems, USA) on a PC. The 3 components of the copepod trajectory were finally extracted using frame analysis, and stored. One should note here that this procedure allows the recording of the coordinates at an even sampling rate (12.5 Hz) that implies no interpolation, and only requires 1 operator. Moreover, no VHS video-cassette recorder is necessary, and only 1 video monitor is sufficient to visualize the 2 orthogonal views.

Each individual *Temora* was recorded swimming for 40 min (the maximum memory size allowed by our frame-disk), after which valid segments were identified for analysis. Here, valid segments consisted of pathways in which the animals were swimming freely, at least 2 body lengths away from any of the chamber's walls or the surface of the water. An illustration of the resulting 3D trajectories is given in fig. 3 (see also Table 1).

Statistical study of zooplankton displacements

Background

We note here that $X(t)$ is the 3D position of the zooplankter at time, t . Now we consider the norm $\|\Delta X_\tau\|$ of its displacements as:

$$\|\Delta X_\tau\| = \left[(x(t+\tau) - x(t))^2 + (y(t+\tau) - y(t))^2 + (z(t+\tau) - z(t))^2 \right]^{1/2}, \quad (1)$$

where τ is the time increment (i.e., the time scale at which the norm is estimated), and $x(t), y(t)$, and $z(t)$ are the 3D coordinates of the zooplankter at time, t . By definition, and as recently illustrated on a set of different behavioral metrics including the distance traveled and the turning angle (Seuront et al. 2004), the norm of the displacements $\|\Delta X_\tau\|$ is scale-dependent. Mathematically, this is called a nonstationary process with stationary increments: the statistics of the increment do not depend on time, t , but only on the time increment, τ . More generally, the moments of order q ($q > 0$ the moments of orders 1 and 2 are the mean and the variance, respectively) can thus be regarded as depending only of the time increment, τ , following

Table 1. Code, duration, and number of data points available from each of the 9 and 14 swimming paths of *Daphnia pulex* and *Temora longicornis* analyzed, respectively

<i>Daphnia pulex</i>			<i>Temora longicornis</i>		
Path	N	Duration	Path	N	Duration
Dp ₁	864	1 mn 26 s	Tl ₁	3022	4 mn 18 s
Dp ₂	2413	4 mn 01 s	Tl ₂	3130	4 mn 10 s
Dp ₃	1892	3 mn 09 s	Tl ₃	2531	3 mn 22 s
Dp ₄	1785	2 mn 58 s	Tl ₄	2278	3 mn 02 s
Dp ₅	1733	2 mn 53 s	Tl ₅	2856	3 mn 48 s
Dp ₆	2277	3 mn 48 s	Tl ₆	1934	2 mn 34 s
Dp ₇	1912	3 mn 11 s	Tl ₇	3579	4 mn 46 s
Dp ₈	1460	2 mn 25 s	Tl ₈	2331	3 mn 06 s
Dp ₉	1479	2 mn 28 s	Tl ₉	2566	3 mn 25 s
-	-	-	Tl ₁₀	2436	3 mn 15 s
-	-	-	Tl ₁₁	3137	4 mn 10 s
-	-	-	Tl ₁₂	2040	2 mn 43 s
-	-	-	Tl ₁₃	3129	4 mn 10 s
-	-	-	Tl ₁₄	3520	4 mn 41 s

(Schmitt and Seuront, 2001 2002):

$$\langle \|\Delta X_\tau\|^q \rangle \approx \left(\frac{\tau}{T} \right)^{\xi(q)} \langle \|\Delta X_T\|^q \rangle; \quad (2)$$

where $\xi(q)$ is the moment function characterizing the fluctuations of the norm, $\|\Delta X_\tau\|$, regardless of the scale and intensity, and T is a characteristic (fixed) large time scale. In other words, the low and high orders of moment, q , characterize smaller (i.e., the more-frequently observed) displacements and larger (i.e., the less-frequent) displacements, respectively.

Diffusion versus anomalous diffusion

The exponent function, $\xi(q)$, can be very useful in characterizing the statistics of the so-called random walk. For Brownian motion, it is well known that $\xi(q)=q/2$. In this framework, only the moment of order 2 is estimated, and whenever $\xi(2)=1$, the process corresponds to normal diffusion, whereas the rich field of anomalous diffusion corresponds to dispersive processes with $\xi(2) \neq 1$ (Castiglione et al. 2000). The idea behind this

characterization using only 1 moment was implicitly to assume that if $\xi(2)=1$, one has for all values of q , $\xi(q)=q/2$ so that the process has the same diffusive properties as Brownian motion. Of course, this is not necessarily the case, and one can have $\xi(2)=1$ (so that the diffusion is apparently normal; see Ferrari et al. 2001), whereas for other moments $\xi(q) \neq q/2$. One should note here that the same general conclusions can be drawn with the more-general fractional Brownian motions defined as $\xi(q)=Hq$, where H is a constant. It is thus better to characterize the process with the entire function, $\xi(q)$, instead of a single exponent (Schmitt and Seuront 2001 2002). In this framework, it would be more coherent to denote "anomalous diffusion" as diffusion with function $\xi(q) \neq q/2$.

When the function $\xi(q)$ is nonlinear, we refer to the resulting diffusion as being "multifractal" (e.g., Seuront et al. 1999) by analogy with multifractal characterization of correlations and intermittency in turbulence (see Andersen et al. 2000 for a recent review). The term "multifractal random walk" has already been proposed in another context (Bacry et al. 2001). Before this, diffusion char-

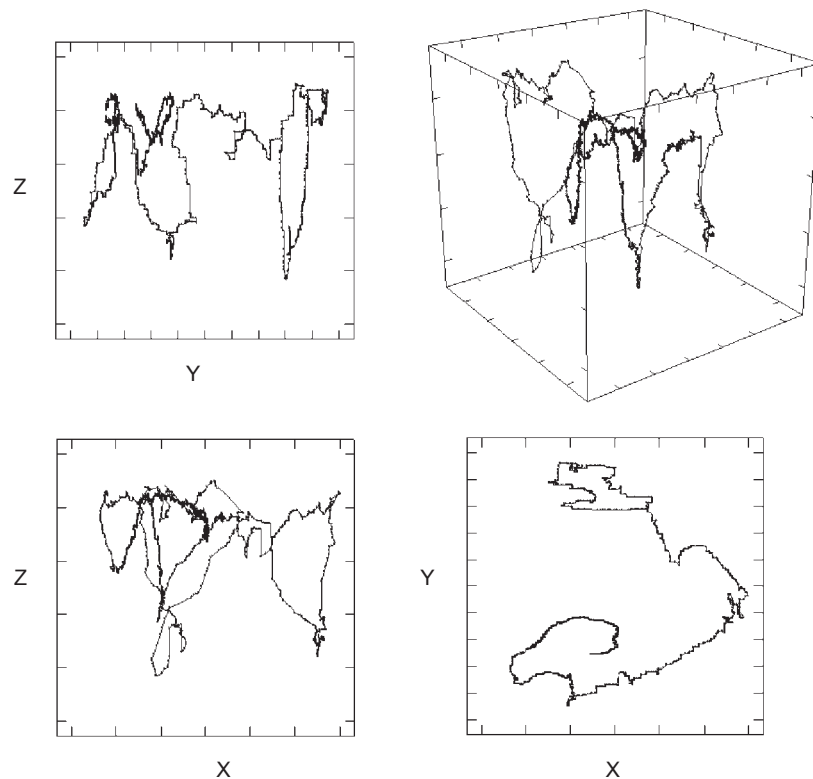


Fig. 2. Three-dimensional swimming pathway of the cladoceran, *Daphnia pulex*, recorded at 10 Hz during 4 min (path Dp₂; see Table 1).

acterized by the nonlinear $\xi(q)$ function was called different names: “generalized diffusion” (Aranson et al. 1990), “multidiffusion” (Sneppen and Jensen 1994), “multifractional kinetics” (Carreras et al. 1999), and “strong diffusion” (Castiglione et al. 1999).

In more practical terms, the multifractal framework, widely applied to the characterization of nutrient, phyto-, and zooplankton patchiness (Seuront et al. 1996a b 1999 2002, Seuront and Lagadeuc 2001, Lovejoy et al. 2001), characterizes positively skewed frequency distributions, reflecting heterogeneous distributions with a few dense patches and a wide range of low-density patches. Now, one has to remember that under the random walk (i.e., normal diffusion) hypothesis, the amplitude of successive displacements, x , follows a Gaussian distribution, in which case, the probability density function decreases as $e^{-x^2/2}$, which is an extremely high rate. In practice, when a swimming path is specifically referred to as being multifractal, high-amplitude displacements are much more frequent than in the random walk case. Furthermore, there is memory in successive displacements, meaning that they are not indepen-

dent as they are for the classical random walk, and a significant long-range correlation exists between them. These properties are responsible for the observed divergence observed in the function $\xi(q)$ between normal diffusion ($\xi(q)=q/2$) and anomalous diffusion ($\xi(q)\neq q/2$, nonlinear and concave).

Practical estimation of function $\xi(q)$

The exponents, $\xi(q)$, are estimated by the slope of the linear trends of $\langle \|\Delta X_\tau\|^q \rangle$ vs. τ in a log-log plot. However, because an objective criterion is needed to decide upon an appropriate range of scales to include in the regressions, we used the values of the time scales which satisfied 2 optimization criteria.

First, we consider a regression window of varying width that ranges from a minimum of 5 data points (the fewest number of data points which ensures the statistical relevance of a regression analysis) to the entire data set. The smallest windows are slid along the entire data set at the smallest available increments, with the entire procedure iterated ($n - 4$) times, where n is the total number of available data points. Within each win-

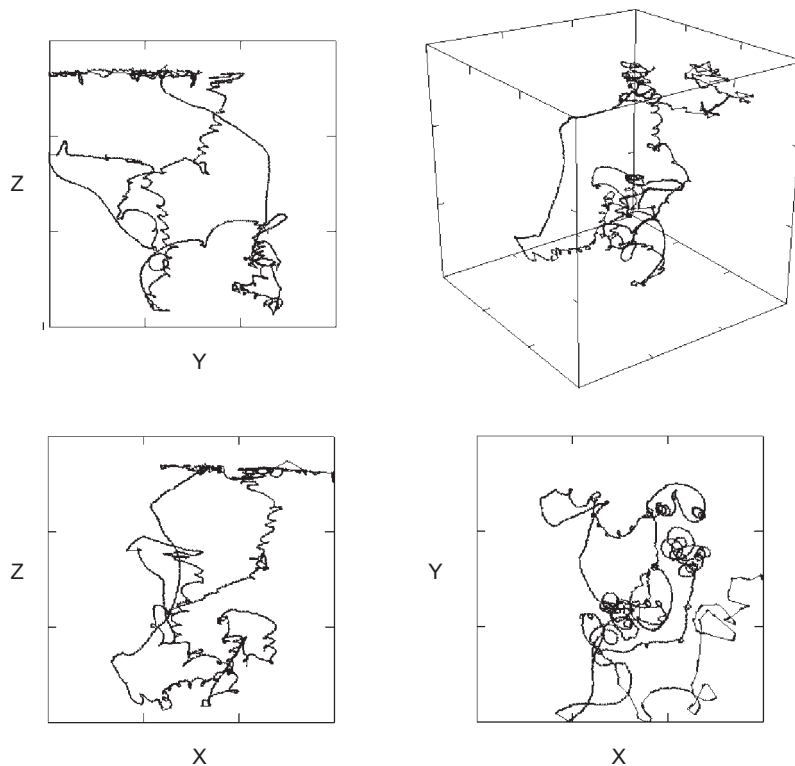


Fig. 3. Three-dimensional swimming pathway of the copepod, *Temora longicornis*, recorded at 12.5 Hz during 4 min 10 s (path T1₁₁; see Table 1).

dow and for each width, we estimate the coefficient of determination (r^2) and the sum of the squared residuals for the regression. We subsequently use the values of τ (Eq. 2) which maximize the coefficient of determination and minimize the total sum of the squared residuals (Seuront and Lagadeuc 1997) to define the scaling range and to estimate the related exponents, $\xi(q)$. Hereafter, this 1st optimization procedure is referred to as the “ R^2 -SSR” criterion.

Second, noting that Eq. (2) can be rewritten as (Seuront et al. 2004)

$$d \log [\langle \|\Delta X_\tau\|^q \rangle] / d \log \tau = \xi(q), \quad (3)$$

it appears that if scaling exists, it will manifest itself as a slope of 0 in plots of $d \log [\langle \|\Delta X_\tau\|^q \rangle] / d \log \tau$ vs. $\log \tau$. Equation (3) can thus be rewritten as

$$d [d \log [\langle \|\Delta X_\tau\|^q \rangle] / d \log \tau] / d \log \tau = 0. \quad (4)$$

As stated above, to ensure the statistical relevance of this procedure, we use a sliding regression window similar to the one described in the “ R^2 -SSR” procedure. The significance of the differences between the slope of each regression and the expected slope line of 0 was directly tested using standard statistical analysis (see Zar 1996). The scaling range was then defined as the scales that statistically verified Eq. (4) and the 1st optimization criterion. Finally, the intercept of the range of scales exhibiting zero-slope behavior provides the exponents’ values for $\xi(q)$ (Eq. 4). Hereafter, this procedure is referred to as the “zero-slope” criterion.

RESULTS

Behavior of free-swimming *Daphnia pulex* and *Temora longicornis*

The 3D records of the swimming behaviors of *Daphnia pulex* and *Temora longicornis* obtained at 10 and 12.5 frames/s are exemplified in figs. 2 and 3, respectively. The 2D projections of these trajectories in the xy , xz , and yz planes are also shown. Both species actively moved in highly fluctuating and irregular ways, alternating between periods of relatively straight and smooth swimming and periods of erratic motions including strong jumps in all 3 dimensions, ensuring the 3D nature of the recorded pathways. This feature was nevertheless clearer for *T. longicornis*. Its trajectory was indeed

characterized by very strong jumps (up to 30 body lengths in 0.08 s), while *D. pulex* only exhibited jumps of 2~3 body lengths in 0.1 s (see also Fig. 1).

We also stress here another difference between the observed behaviors of these 2 species. Indeed, it can be seen from the 2D projections of the 3D swimming paths that the swimming behavior of *D. pulex* was smoother and more regular in the xy plane than in the 2 vertical ones. In contrast, the swimming path of *T. longicornis* seemed to be more isotropic, with the same macroscopic structure in all 3 dimensions.

These observations are investigated, both qualitatively and quantitatively, more thoroughly in the next section.

Multifractal properties of *Daphnia pulex* and *Temora longicornis* displacements

We first consider the properties of both *D. pulex* and *T. longicornis* swimming paths in a 3D space, and second we focus on the 2D projections of these trajectories in the xy , xz , and yz planes. This may be of prime interest (i) to ensure the reliability of comparing results obtained from 2D and 3D experimental procedures and (ii) to investigate potential differential behaviors.

Three-dimensional displacements

The analysis of the 3D trajectories of zooplankton displacements of figs. 2 and 3 is shown in figs. 4A and 5A. The scaling is very good for a range of scales of 2 decades for both species. More specifically, this scaling manifests itself for *D. pulex* and *T. longicornis* for time scales ranging from 0.6 to 40 s and from 0.3 to 30 s, respectively. Considering the mean swimming speed of *D. pulex* and *T. longicornis* (2.4 and 1.3 mm/s), the corresponding distances respectively vary between 1.45 and 96, and 0.4 and 39.0 mm. Practically, that means that the amplitude of displacements bounded between 1.45 and 96 mm for *D. pulex*, and 0.4 and 39.0 mm for *T. longicornis* are structured in a scale-dependent (i.e., scaling) way. In other words, knowledge of the distribution of the smallest displacements is sufficient to infer that of the largest displacements. Finally, we stress here that both the departure from scaling for small time scales and slight differences observed between this departure for *D. pulex* and *T. longicornis* can be related to differential, species-specific reaction times. Thus a species with a fast reaction time is better able to maintain the scaling structure of its

displacements for smaller displacements than a species with a slower reaction time without being subject to contamination of its swimming path by external processes such as turbulent diffusion, microscale shear, or localized changes in viscosity.

Now, to investigate the nature of a potential departure from normal diffusion in *D. pulex* and *T. longicornis* swimming paths, the previous scaling behaviors are compensated for by the normal diffusion scaling exponent, $\tau^{q/2}$. In other words, in cases of normal diffusion, Eq. (2) is written as

$$\langle \|\Delta X_\tau\|^q \rangle \approx \left(\frac{\tau}{T}\right)^{q/2} \langle \|\Delta X_T\|^q \rangle \quad (5)$$

and compensation by the normal diffusion scaling exponent, $\tau^{q/2}$, leads to rewriting Eq. (2) as

$$\langle \|\Delta X_\tau\|^q \rangle / \left(\frac{\tau}{T}\right)^{q/2} \approx \left(\frac{\tau}{T}\right)^{K(q)} \langle \|\Delta X_T\|^q \rangle \quad (6)$$

where $K(q)$ is the compensated exponent function that verifies $K(q)=0$ in case of normal diffusion, regardless of the values of the moment, q . In other words, a log-log plot of $\langle \|\Delta X_\tau\|^q \rangle / \tau^{q/2}$ versus τ should exhibit a flat behavior (i.e., $K(q)=0$). The range of scales used to estimate the compensated function, $K(q)$, was chosen using the “ R^2 -SSR” and “zero-slope” criteria defined above. The resulting compensated scalings (Figs. 4B, 5B) show that function $K(q)$ greatly differs from the normal diffusion case of $K(q)=0$, for behaviors of both *D. pulex* and *T. longicornis*. This confirms the scaling ranges presented above, and indicates the anomalous diffusive character of the swimming behavior of the 2 species investigated here. Moreover, it appears that function $K(q) \neq 0$ even for the lowest values of the moment q for *D. pulex* (Fig. 4B), while this difference becomes perceptible for moments $q > 2$ for *T. longicornis* (Fig. 5B). The frequency distributions of successive displacements then significantly differ from a random walk even with the smallest displacements by *D. pulex*. Alternatively, the smallest displacements of *T. longicornis* can reasonably be thought of as following a random walk. More specifically, this suggests that the swimming behaviors of *D. pulex* and *T. longicornis* correspond to 2 different types of anomalous diffusion. This is confirmed below by analysis of the exponent function, $\zeta(q)$.

The nonlinearity and convexity of function $\zeta(q)$, compared to the linear behavior, i.e., $\zeta(q)=q/2$,

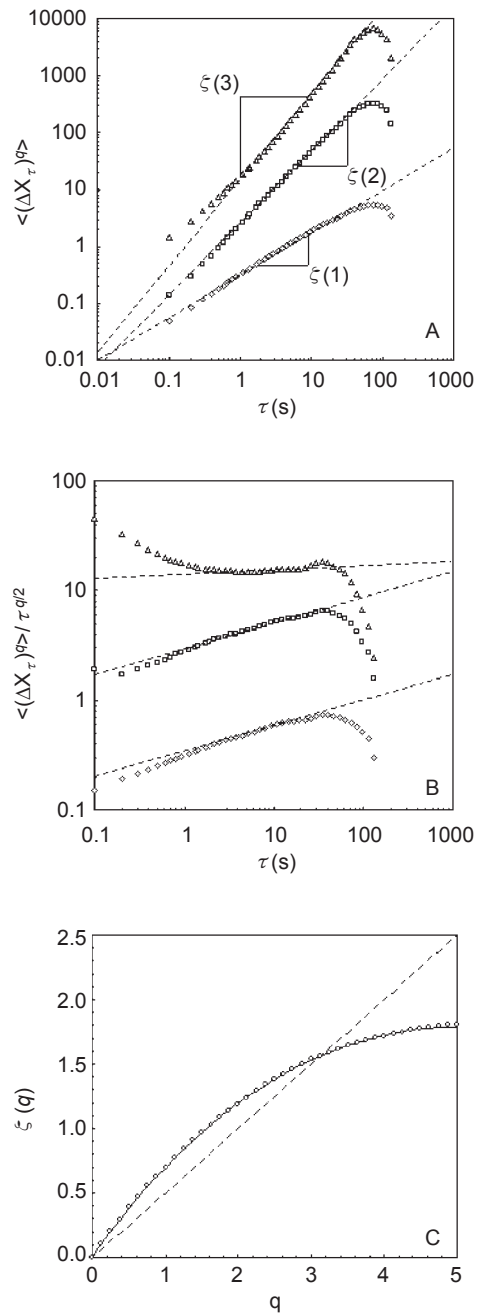


Fig. 4. Moment, $\langle \|\Delta X_\tau\|^q \rangle$, and the compensated moment, $\langle \|\Delta X_\tau\|^q \rangle / \tau^{q/2}$, vs. τ for $q=1, 2$, and 3 (from bottom to top) in log-log plots (A and B, respectively), computed from the swimming path, Dp_2 (see Table 1), of the cladoceran, *Daphnia pulex*. The scaling of the moments (A) is very good over 2 decades, ranging from 0.6 to 40 s. This is confirmed by the scaling of the residual (B) that indicates anomalous diffusion (i.e., a slope differing from 0) over a similar range of scales. (C) Function $\zeta(q)$ estimated as the slope of the linear trends of $\langle \|\Delta X_\tau\|^q \rangle$ vs. τ in a log-log plot, compared to a fit corresponding to normal diffusion ($\zeta(q)=q/2$, dotted line). The nonlinearity and convexity of the empirical curve are indicative of multifractality.

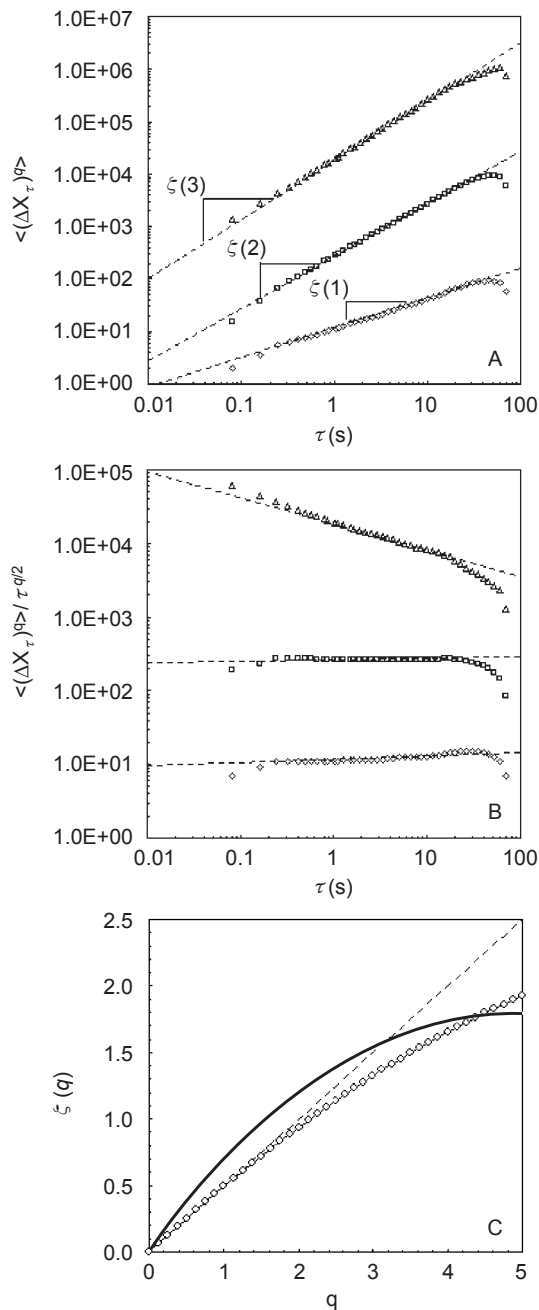


Fig. 5. Moment, $\langle \|\Delta X_\tau\|^q \rangle$, and the compensated moment, $\langle \|\Delta X_\tau\|^q \rangle / \tau^{q/2}$, vs. τ for $q=1, 2$, and 3 (from bottom to top) in log-log plots (A and B, respectively), computed from the swimming path TI_{11} (see Table 1) of the copepod *Temora longicornis*. The scaling of the moments (A) is very good over 2 decades, ranging from 0.3 to 30 s. This is confirmed by the scaling of the residual (B) that indicates anomalous diffusion (i.e., slope differing from 0) over a similar range of scales. (C) Function $\xi(q)$ estimated as the slope of the linear trends of $\langle \|\Delta X_\tau\|^q \rangle$ vs. τ in a log-log plot, compared to a fit corresponding to normal diffusion ($\xi(q)=q/2$, dotted line). The nonlinearity and convexity of the empirical curve are indicative of multifractality. Function $\xi(q)$ estimated from *Daphnia pulex* 3D behavior is shown for comparison (thick continuous gray curve).

expected in cases of normal diffusion, indicates the multifractal nature of the swimming paths of both *D. pulex* and *T. longicornis* (Figs. 4C, 5C). As suggested above, the departure from linearity is very strong for *D. pulex*, even for low values of moment q (Fig. 4C), while for *T. longicornis*, this departure is very clear only for moments larger than 2 (Fig. 5C). This confirms, first, the anomalous diffusive characters of the swimming behaviors of *D. pulex* and *T. longicornis*, and second, the species-specific nature of the so-called multifractal random walk shown here. We indeed see in Figs. 4C and 5C that the 2 curves markedly differ for the 2 species, since the curvature for *D. pulex* is much more pronounced than that for *T. longicornis*. Furthermore, while $\xi(2) \approx 1$ for the latter, $\xi(2)$ is clearly larger than 1 for the former. Let us remember that diffusion is often characterized by the diffusivity, Γ , defined as :

$$\langle \Delta X_\tau^2 \rangle \approx \Gamma \tau. \quad (7)$$

Within our scaling framework, whenever $\xi(2) \neq 1$, the diffusivity is scale-dependent and obeys the law, $\Gamma(\tau) \approx \tau^{\xi(2)-1}$. Here, the diffusivity for *T. longicornis* is almost scale-independent, whereas the diffusivity for *D. pulex* is clearly scale-dependent. In this case, even a 2nd-order analysis would reveal anomalous diffusion.

Two-dimensional displacements

Analysis of the 2D components of the initial 3D swimming paths leads to further results (Fig. 6). We thus show clear differences between *D. pulex* and *T. longicornis*. The multifractal properties of the swimming path of *T. longicornis* are very similar in 2 and 3 dimensions (Fig. 6A). The swimming behavior of *T. longicornis* can then be thought as being isotropic. On the contrary, *D. pulex* presents differential behavior in 2 and 3 dimensions. Function $\xi(q)$ estimated from the projection in the xy plane has the same shape as the original 3D one. Alternatively, function $\xi(q)$ estimated from projections in the xz and yz planes diverges from the 3D one for moments $q > 3$ (Fig. 6B).

DISCUSSION

Multifractal scaling exponents reveal an optimization strategy of zooplankton

We here interpret the nonlinearity of the expo-

ment $\xi(q)$ in the framework of a foraging strategy using Eq. (6). Let us first recall that large q values are associated with large displacements, whereas small q values characterize small displacements. For small time scales (and hence small distances), and large q , the ratio $(\tau/T)^{K(q)}$ is large, showing that there are more large displacements for the multifractal random walk ($K(q)>0$) than for the classical random walk ($K(q)=0$). On the other hand, for small q , $K(q)<0$, so that the ratio $(\tau/T)^{K(q)}$ is small, and the multifractal random walk has fewer small displacements compared to the classical random walk. For larger time scales, when τ is close to the largest scale T of the system, the ratio $(\tau/T)^{K(q)}$ is close to 1, so that the difference between the multifractal random walk and classical random walk is less perceptible. This discussion shows that the scaling multifractal function, $\xi(q)$, characterizes (i) in a scale-invariant way, exploration of the volume by the plankter, and (ii) for large and

small moments, a type of optimization of this exploration. This may explain why this $\xi(q)$ function is likely to be species dependent and hence strategy dependent.

Comparing zooplankton behavior with the structure of the surrounding environment

The results presented here have several salient implications for our understanding of zooplankton behavior and trophodynamics. In particular, the multifractal statistics observed in the behaviors of both *Daphnia pulex* and *Temora longicornis* are reminiscent of the multifractal (i.e., patchy) distributions found for phytoplankton under different turbulence intensities (e.g., Seuront et al. 1999, Lovejoy et al. 2001, Seuront and Schmitt 2001). Considering the remote-sensing ability of zooplankton organisms, their behaviors can be strongly influenced by the distribution of their phytoplanktonic prey. Ultimately, knowledge of the precise nature of zooplankton swimming behavior can then be a way to infer the spatial distribution of prey.

Two-dimensional versus 3D fractal dimension estimates

The absence of clearly defined differential modes of swimming behavior of *T. longicornis* (cf. Fig. 6A) in the horizontal and vertical dimensions suggests the absence of a feeding switch between 2 different kinds of food sources as with the non-motile alga *Nannochloropsis oculata* and the motile flagellate *Oxyrrhis marina* used in the present study. Considering the evidence for prey-switching behavior (e.g., Kjørboe et al. 1996, Caparroy et al. 1998), multifractal analysis is thus suggested as a diagnostic framework to determine the kind of prey zooplankton preferentially feed on in a pluri-specific prey assemblage. On the contrary, identification of different modes of swimming behavior for *D. pulex* (see Fig. 6B) in the vertical and horizontal dimensions may reflect (i) their characteristic hop-and-sink behavior that intrinsically imparts differential importance to the horizontal and vertical dimensions, (ii) the effect of gravity which affects most zooplankton species (Strickler 1982), and (iii) a reminiscence of diel vertical migration as a predator-avoidance strategy (Loose 1992, Loose et al. 1992). Differential swimming behaviors in the horizontal and vertical planes may finally also be suggested as a potential basis for investigating the predation risk associated with dif-

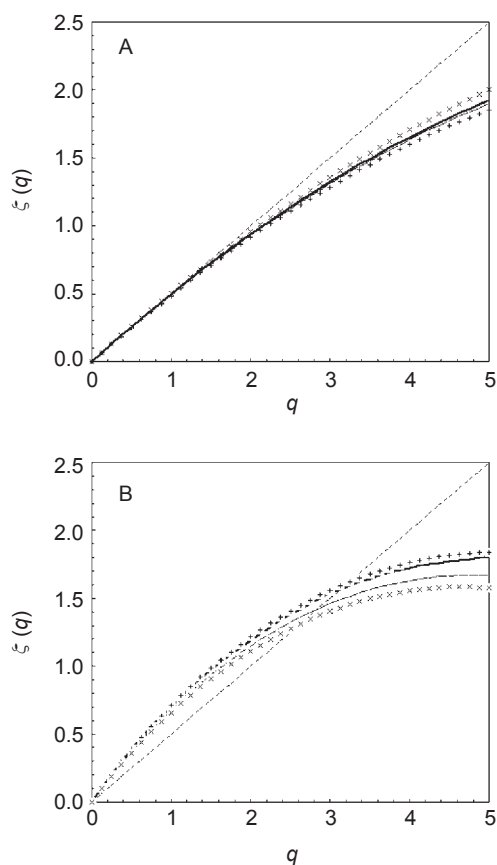


Fig. 6. Function $\xi(q)$ estimated from *Temora longicornis* (A) and *Daphnia pulex* (B) swimming paths Π_{11} and Dp_2 , respectively (see Table 1). Function $\xi(q)$ estimated from the initial 3D paths (continuous curve) is compared to the functions obtained from their 2D projections on the $xy(+)$, $yz(-)$, and $xz(x)$ planes.

ferential swimming behaviors related to mating, feeding, or predator-avoidance strategies. Moreover, this result is fully congruent with the higher fractal dimension found for the vertical component of *D. pulex* swimming behavior (Seuront et al. 2004). Indeed, an increase in the fractal dimension, D , is equivalent to a decrease in the scaling exponent, $\xi(2)$ (see Seuront et al. 2002 for further details). Depending on the relative velocities of predator and prey, a swimming behavior characterized by a high fractal dimension, i.e., a low $\xi(2)$, may imply a high encounter probability with predators, relative to more-linear swimming paths.

Individual behaviors affect the outcomes of predator-prey interactions, especially in the pelagic environment, where prey movement is important both as a cue to predators (Brewer and Coughlin 1995) and a determinant of the encounter rate (Gerritsen and Strickler 1977). Moreover, the distribution of prey organisms is very important for predators, as recently investigated numerically (Seuront 2001, Seuront et al. 2001), because food availability changes depending on its distribution. If a predator can remotely detect its surroundings, patchy prey distributions should be more efficient. In contrast, when a predator has no remote detection ability, more-homogeneous prey distributions should be relatively better, because available food quantity or the encounter rate becomes proportional to the searched volume as patchiness decreases. Moreover, the very complex patchy structure associated with a multifractal distribution may also change the nature of the food signal, usually regarded as being homogeneously distributed in space and time in models of predator-prey encounter rates. Indeed, planktonic animals have been shown to remain within patches when feeding (Price 1989), or to exhibit more fine-scale movements in areas of higher food concentration (Bundy et al. 1993). Encounter rates might greatly differ when organisms feed within patches (intensive searching) as opposed to searching for new patches (extensive searching), and their related behaviors should be more and less complex, respectively. Extrapolating this reasoning to random walk and multifractal random walk, intensive and extensive searches might then be related to swimming behavior which increasingly diverges from random walk. Foraging models likely incorporate switching between feeding and searching behaviors as scaled to organism size, in order to effectively simulate these complex physical-biological relationships (Seuront and Lagadeuc 2001). This was also interpreted above in the framework

of optimization of the foraging strategy in multi-scale patches. Comparison of the multifractal nature of plankton swimming behavior and plankton distributions will then increase our understanding of zooplankton trophodynamics. In particular, in the ocean, which is increasingly regarded as a "seascape" considering the growing awareness of the heterogeneous nature of microscale processes (e.g., Seymour et al. 2000, Waters and Mitchell 2002, Waters et al. 2003), behavioral studies will be of prime interest for improving our understanding of the functioning of marine ecosystems from a bottom-up view (Seuront 2001, Seuront et al. 2001).

CONCLUSIONS

We stress here that an important consequence of the multifractal nature of zooplankton swimming behavior, illustrated using the 3D swimming paths of *Daphnia pulex* and *Temora longicornis*, is its deviation from Brownian motion and fractional Brownian motion. While these latter 2 have been suggested for characterizing the movement of organisms (Frontier 1987), Wiens and Milne (1989) found that observed beetle movements deviated from the modeled fractional Brownian motion. A follow-up study by Johnson et al. (1992) found that beetle movements reflect a combination of normal and anomalous diffusions.

While an extensive discussion of the anomalous diffusion of copepods in a multifractal environment can be found elsewhere (Marguerit et al. 1998, Schmitt and Seuront 2001), it is suggested here that multifractal analysis might become an efficient diagnostic tool to access the detailed nature of zooplankton swimming behaviors, in particular for identifying differential swimming behaviors in different spatial directions. Future modeling attempts of zooplankton swimming behavior may also have to take into account the multifractal character of an organism's movements as recently suggested by Schmitt and Seuront (2001 2002).

Acknowledgments: The authors are indebted to Dr. L. Falk and Dr. H. Vivier for letting us use their lab facilities (Laboratory of Chemical Engineering Sciences, ENSIC, UPR CNRS 6811, Nancy, France); to Dr. P. Pitiot for his priceless help in data acquisition and preprocessing; and to Ms. V. Denis for technical assistance. Thanks are extended to the captain and the crew of the *NO Sepia II* for their help during the sampling experi-

ments; to Prof. Y. Lagadeuc for initiating collaboration with the Laboratory of Chemical Engineering Sciences; and to S. Leterme for her help in the final formatting of the manuscript. We thank 4 anonymous reviewers for constructive criticisms of an earlier version of this work. This work is a contribution of the Ecosystem Complexity Research Group.

REFERENCES

- Andersen KH, P Castiglione, A Mazzanino, A Vulpiani. 2000. On strong anomalous diffusion. *Physica D* **134**: 75-93.
- Aranson IS, MI Rabinovich, LS Tsimring. 1990. Anomalous diffusion of particles in regular fields. *Phys. Lett. A* **151**: 523-528.
- Bacry E, J Delour, JF Muzy. 2001. A multifractal random walk. *Phys. Rev. E* **64**: 103-106.
- Bascompte J, C Vilà. 1997. Fractals and search paths in mammals. *Land. Ecol.* **12**: 213-221.
- Brewer MC. 1996. *Daphnia* swimming behavior and its role in predator-prey interactions. PhD thesis, Univ. of Wisconsin-Milwaukee, 155 p.
- Brewer MC, JN Coughlin. 1995. Virtual plankton: a novel approach to the investigation of aquatic predator-prey interactions. *Mar. Freshw. Behav. Phy.* **26**: 91-100.
- Bundy MH, TF Gross, DJ Coughlin, JR Strickler. 1993. Quantifying copepod searching efficiency using swimming pattern and perceptive ability. *Bull. Mar. Sci.* **53**: 15-28.
- Caparroy P, MT Pérez, F Carlotti. 1998. Feeding behaviour of *Centropages typicus* in calm and turbulent conditions. *Mar. Ecol.-Prog. Ser.* **168**: 109-118.
- Carreras BA, VE Lynch, DE Newman, GM Zaslavsky. 1999. Anomalous diffusion in a running sandpile model. *Phys. Rev. E* **60**: 4770-4778.
- Castiglione P, A Mazzino, P Muratore-Ginanneschi. 2000. Numerical study of strong anomalous diffusion. *Physica A* **280**: 60-68.
- Castiglione P, A Mazzino, P Muratore-Ginanneschi, A Vulpani. 1999. On strong anomalous diffusion. *Physica D* **134**: 75-93.
- Cody ML. 1971. Finch flocks in the Mohave desert. *Theor. Popul. Biol.* **163**: 161-172.
- Coughlin DJ, JR Strickler, B Sanderson. 1992. Swimming and search behaviour in clownfish, *Amphiprion perideraion*, larvae. *Anim. Behav.* **44**: 427-440.
- Cowles TJ, RA Desiderio, ME Carr. 1998. Small-scale planktonic structure: persistence and trophic consequences. *Oceanography* **11**: 4-9.
- Dowling NA, SJ Hall, JG Mitchell. 2000. Foraging kinematics of *barramundi* during early stages of development. *J. Fish Biol.* **57**: 337-353.
- Erlandson J, V Kostylev. 1995. Trail following, speed and fractal dimension of movement in a marine prosobranch, *Littorina littorea*, during a mating and a non-mating season. *Mar. Biol.* **122**: 87-94.
- Ferrari R, AJ Manfroi, WR Young. 2001. Strongly and weakly self-similar diffusion. *Physica D* **1545**: 111-137.
- Frontier S. 1987. Applications of fractal theory to ecology. In P Legendre, L Legendre, eds. *Developments in numerical ecology*. Berlin: Springer, pp. 335-378.
- Gautestad AO, I Mysterud. 1993. Physical and biological mechanisms in animal movement processes. *J. Appl. Ecol.* **30**: 523-535.
- Gerritsen J, JR Strickler. 1977. Encounter probabilities and community structure in zooplankton: a mathematical model. *J. Fish. Res. Board Can.* **34**: 73-82.
- Johnson AR, BT Milne, JA Wiens. 1992. Diffusion in fractal landscapes: simulations and experimental studies of tenebrionid beetle movements. *Ecology* **73**: 1968-1983
- Jonsson PR, M Johansson. 1997. Swimming behaviour, patch exploitation and dispersal capacity of a marine benthic ciliate in flume flow. *J. Exp. Mar. Biol. Ecol.* **215**: 135-153.
- Kjørboe T, E Saiz, M Viitasalo. 1996. Prey switching behaviour in the planktonic copepod *Acartia tonsa*. *Mar. Ecol.-Prog. Ser.* **143**: 65-75.
- Lampert W. 1987. Feeding and nutrition in *Daphnia*. *Mem. Del. Inst. Ital. Di Idrol.*, 143-192.
- Loose CJ. 1992. *Daphnia* diel vertical migration behavior: response to vertebrate predator abundance. *Arch. Hydrobiol. Beih.* **39**: 29-36.
- Loose CJ, E Von Elert, P Dawidowicz. 1992. Chemically-induced diel vertical migration in *Daphnia*: a new bioassay for kairomones exuded by fish. *Arch. Hydrobiol.* **126**: 329-337.
- Lovejoy S, WJS Currie, Y Tessier, MR Claereboudt, E Bourget, JC Roff, D Schertzer. 2001. Universal multifractals and ocean patchiness: phytoplankton, physical fields and coastal heterogeneity. *J. Plankton Res.* **23**: 117-141.
- Marguerit C, D Schertzer, F Schmitt, S Lovejoy. 1998. Copepod diffusion within multifractal phytoplankton fields. *J. Marine Syst.* **16**: 69-83.
- Mouillot D, D. Viale. 2001. Satellite tracking of a fin whale (*Balaenoptera physalus*) in the north-western Mediterranean Sea and fractal analysis of its trajectory. *Hydrobiologia* **452**: 163-171.
- Peitgen HO, H Jürgensand, D Saupe. 1992. *Fractals for the classroom*. New York: Springer.
- Price HJ. 1989. Feeding mechanisms of krill in response to algal patches: a mesocosm study. *Limnol. Oceanogr.* **34**: 649-659.
- Pyke GH. 1981. Optimal foraging in hummingbirds: rule of movement between inflorescences. *Anim. Behav.* **29**: 882-896.
- Schmitt F, L Seuront. 2001. Multifractal random walk in copepod behavior. *Physica A* **301**: 375-396.
- Schmitt F, L Seuront. 2002. Multifractal anomalous diffusion in swimming behavior of marine organisms. In Y Pomeau, R Ribotta, eds. *Proc. 5th Rencontre du Non-linéaire*, Paris, Institut Poincaré. Paris: Non-linéaire Publications, pp. 237-242.
- Seuront L. 2001. Microscale processes in the ocean: Why are they so important for ecosystem functioning? *La Mer* **39**: 1-8.
- Seuront L, MC Brewer, JR Strickler. 2004. Quantifying zooplankton swimming behavior: the question of scale. In L Seuront, PG Strutton, eds. *Handbook of scaling methods in aquatic ecology: measurement, analysis, simulation*. Boca Raton, FL: CRC Press, pp. 333-359.
- Seuront L, V Gentilhomme, Y Lagadeuc. 2002. Small-scale nutrient patches in tidally mixed coastal waters. *Mar. Ecol.-Prog. Ser.* **232**: 29-44.
- Seuront L, Y Lagadeuc. 1997. Characterisation of space-time variability in stratified and mixed coastal waters (Baie des Chaleurs, Québec, Canada): application of fractal theory. *Mar. Ecol.-Prog. Ser.* **159**: 81-95.

- Seuront L, Y Lagadeuc. 2001. Multiscale patchiness of the calanoid copepod *Temora longicornis* in a turbulent coastal sea. *J. Plankton Res.* **23**: 1137-1145.
- Seuront L, F Schmitt. 2001. Describing intermittent processes in the ocean-univariate and bivariate multiscaling procedures. *In* P Muller, C Garrett, eds. *Stirring and mixing in a stratified ocean*. Proceedings of "Aha Huliko" a Hawaiian Winter Workshop, SOEST, Univ. of Hawaii, pp.129-144.
- Seuront L, F Schmitt, Y Lagadeuc. 2001. Turbulence intermittency, phytoplankton patchiness and encounter rates in plankton: Where do we go from here? *Deep-Sea Res. PT. I* **48**: 1199-1215.
- Seuront L, F Schmitt, Y Lagadeuc, D Schertzer, S Lovejoy. 1999. Universal multifractal analysis as a tool to characterize multiscale intermittent patterns: example of phytoplankton distribution in turbulent coastal waters. *J. Plankton Res.* **21**: 877-922.
- Seuront L, F Schmitt, Y Lagadeuc, D Schertzer, S Lovejoy, S Frontier. 1996b. Multifractal analysis of phytoplankton biomass and temperature in the ocean. *Geophys. Res. Lett.* **23**: 3591-3594.
- Seuront L, F Schmitt, D Schertzer, Y Lagadeuc, S Lovejoy. 1996a. Multifractal intermittency of Eulerian and Lagrangian turbulence of ocean temperature and plankton fields. *Nonlinear Proc. Geophys.* **3**: 236-246.
- Seymour JR, JG Mitchell, L Pearson, RL Waters. 2000. Heterogeneity in bacterioplankton abundance from 4,5 millimetre resolution sampling. *Aquat. Microb. Ecol.* **22**: 143-153.
- Sneppen K, MH Jensen. 1994. Multifractal in critical dynamics of strings and membranes. *Phys. Rev. E* **49**: 919-922.
- Strickler JR. 1982. Calanoid copepods, feeding currents, and the role of gravity. *Science* **218**: 158-160.
- Strickler JR. 1985. Feeding currents in calanoid copepods: two new hypotheses. *Symp. Soc. Exp. Biol.* **39**: 459-485.
- Van Ballemberghe V. 1983. Extraterritorial movements and dispersal of wolves in southcentral Alaska. *J. Mammal.* **64**: 168-171.
- Waters RL, JG Mitchell. 2002. The centimetre-scale spatial structure of estuarine in vivo fluorescence profiles. *Mar. Ecol.-Prog. Ser.* **237**: 51-63.
- Waters RL, JG Mitchell, JR Seymour. 2003. Geostatistical characterization of centimetre-scale spatial structure of in vivo fluorescence. *Mar. Ecol.-Prog. Ser.* **251**: 49-58.
- Wiens JA, TO Crist, KA With, BT Milne. 1995. Fractal patterns of insect movement in microlandscape mosaics. *Ecology* **76**: 663-666.
- Wiens JA, BT Milne. 1989. Scaling of "landscapes" in landscape ecology, or landscape ecology from a beetle's perspective. *Land. Ecol.* **3**: 87-96.
- Zar JH. 1996. *Biostatistical analysis*. Englewood Cliffs, NJ: Prentice Hall International.